Journal of MATERIALS RESEARCH

Article
DOI: 10.1557/jmr.2019.161

Development of new polyimide powder for selective laser sintering

Gleb Vaganov[1,a)], Andrey Didenko[1], Elena Ivan'kova[1], Elena Popova[1], Vladimir Yudin[1], Vladimir Elokhovskii[1], Irena Lasota[2]

[1]*Laboratory of Polymer Mechanics and Composite Materials, Institute of Macromolecular Compounds Russian Academy of Science, St. Petersburg 199004, Russia*
[2]*Department of Research and Development in the field of Laser and Hybrid Laser-Arc Technology, Peter the Great Saint-Petersburg Polytechnic University, St. Petersburg 195251, Russia*
[a)]Address all correspondence to this author. e-mail: glebvaganov@mail.ru

Received: 31 January 2019; accepted: 18 April 2019

A comparative study of properties of the films based on polyimide powders synthesized by chemical or thermal imidization is presented. It is shown that the imidization method affects the shape, size, bulk density, and size distribution of the synthesized polyimide powder particles, which influences the properties of the films obtained. The method of chemical modification allows to obtain denser powders comparing to the thermally imidized powder. The films were obtained with the help of selective laser sintering (SLS) for the first time. It is shown that the films produced by SLS from chemically imidized polyimide powder are more dense and monolithic as compared to those made from thermally imidized polyimide, which provides, obviously, higher mechanical characteristics of the former. They have the strength higher in 2.5 times and the elastic modulus twice as high than latter one. The optimal laser power is 65 W.

Introduction

The additive technology or layer-by-layer creation of materials is increasing in importance. This is the creation of a computer model of the future part and the receipt of the product itself by adding material on a layer-by-layer basis using special equipment [1].

One of the most promising representatives of additive technology for obtaining high-quality products from metals, their alloys, ceramics, and polymers is a technology based on the growth of work pieces and parts using the selective laser sintering (SLS). The principle of the products formation by this technology consists in the layer-by-layer growing of the product followed by sintering the powder material. As a result, it is possible to obtain parts of complex shape, which are simply impossible to manufacture using conventional casting methods. The use of such new methods helps to reduce material consumption and increase productivity [1].

The main advantages of SLS over other technologies of additive production are the following [2]: (i) products produced by the SLS method are similar in properties of polymeric materials obtained using standard methods such as extrusion, injection molding, and hot pressing; (ii) theoretically, any material that can be transferred in a powder state and melted at increasing temperature can be processed using SLS technology; (iii) the absence of any additional supporting element when printing complex products.

The properties of the final product obtained by the SLS technology largely depend on the properties of the original powder (morphology, size, size distribution, bulk density, thermal properties, viscosity, and surface tension) and on the parameters of laser sintering (laser power, scanning speed, and laser spot diameter) [3]. Particle morphology affects the spatial arrangement of powder particles (stacking degree) relative to each other. Spherical (with a smooth surface) particles have a high packing density. They provide flowability of the powder composition in systems of applying the material with minimal resistance. In addition, spherical particles are well-bonded in the process of laser sintering. It was shown that during the transition from powder particles with predominantly spherical morphology to particles of irregular shape of the same material, the elastic modulus decreases by almost 40% [3]. The spherical particles with good flowability and high packing densities represent ideal characteristics of the starting powder for use in SLS [4]. At the same time, the use of irregularly shaped particles with a large

https://doi.org/10.1557/jmr.2019.161 Published online by Cambridge University Press

© Materials Research Society 2019

variation in their size leads to the creation of products with higher mechanical characteristics, compared to the use of mainly spherical particles with a narrow size distribution [5].

Nowadays, SLS technology is applied to polyamides such as polyamide 12 [5, 6, 7], polyamide 11 [8, 9], and also polyamide 6 [10].

The mechanical properties of the material obtained by SLS technology using polyamide powders are similar to the products obtained by injection molding, but with lower deformation at break. The samples obtained by this way can be used not only to create injection molds and prototypes but also to obtain functional products [11].

Research on the application of other polymers in SLS technology is very limited. In addition to polyamide, polystyrene and polycarbonate are used as a starting material for SLS [12, 13].

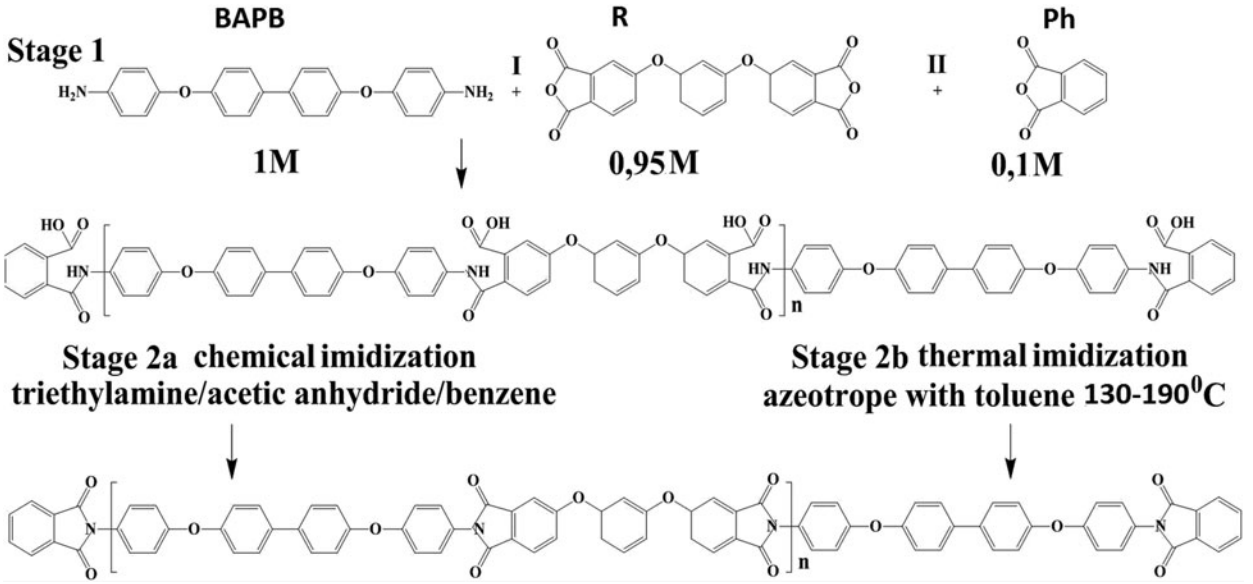
Currently, various industries (such as aerospace, automotive, and medical) have shown increased interest in manufacturing of products using the SLS method for the production of high-strength, heat-resistant polymeric materials. Among heat-resistant polymers, research and application of SLS technology is focused on the family of polyaryletherketone (PAEK), in particular on polyetherketone (PEK) [14, 15] and polyetheretherketone (PEEK) [16, 17]. At the same time, materials obtained by SLS based on PEEK are used not only for the creation of high-strength heat-resistant products but also for creating scaffolds in tissue engineering [16, 17].

Analysis of the modern literature has shown that today there are quite extensive studies in the use of standard thermoplastic polymeric materials, mainly based on polyamide, in SLS. At the same time, there are noticeably fewer studies in the field of application of heat-resistant polymers for SLS, all of the currently published works in this area are focused only on the PAEK family. Thus, at the moment, there is no information about the use of other classes of heat-resistant polymers, for example, polyimides. In this regard, from a scientific and technical point of view, it is interesting and promising to study the patterns of structure formation during SLS of polyimide powders and to study the process of their fusion depending on the structure and properties of the powder, as well as parameters of SLS.

Results and discussion

A semi-crystalline polyimide based on resorcinol dianhydride R and tetracyclic diamine BAPB was synthesized by chemical and thermal imidization (Scheme 1). The synthesized polyimide had an average molecular weight of $M_w \sim$ 13,000 determined by the method of light scattering [18]. In earlier publications, the composition and structure of polyimide was shown by IR-spectroscopy and NMR analysis [19, 20]. In the IR-spectrum, there were bands corresponding to the five-membered imide cycle: a doublet in the region of 1720–1780 cm^{-1} and a band at 720 cm^{-1}. Thus, we can say that the chemical composition and structure of the polyimide obtained by thermal and by chemical imidization techniques are analogues.

DSC is a powerful method to characterize the melting and crystallization behavior of semi-crystalline plastics. There are two parameters, which are of special interest for the laser sintering process. The first important parameter—the window of sinterability—is the difference between the onset



Scheme 1: Synthesis of polyimides R-BAPB by the methods of thermal and chemical imidization.

https://doi.org/10.1557/jmr.2019.161 Published online by Cambridge University Press

© Materials Research Society 2019

temperatures of the melting (T_m) and crystallization peak [19]. This window delimits the temperature range of the powder layer. Since the sintering of particles occurs under the action of a laser on a thin powder layer, for formation of the required level of adhesion between the layers, it is necessary that the lower layer would not have time to crystallize until the subsequent layer is applied. Generally, the wider the sinterability window, the easier the control of the sintering process.

The second parameter—the degree of crystallinity of the used material—is represented by the area below the melting peak of the sample. In this case, the lower crystallinity leads to the lower shrinkage and the better dimensional accuracy of the sample.

The results obtained during the first heating of the studied polyimide powders are shown in Table I. Both polyimide powders had endothermic melting peaks with a temperature of ~318 °C, which indicates that the polyimide powders were crystalline, while the specific thermal transitions corresponding to T_g were not observed (Fig. 1). The glass transition temperatures were determined only by reheating the powders. When the powders were cooled from 360 °C to 30 °C, no crystallization was observed (Fig. 1). It is known that for the crystallization of this polyimide, an additional exposure at a temperature of 280 °C for 1 h is necessary [21]. Since the SLS process is too fast, it takes seconds to create a single layer. Therefore, during such a short period of time, polyimide samples do not have enough time to crystallize and remain in amorphous state after laser sintering. Such a feature of this polyimide, namely slow crystallization, plays a positive role in the SLS process, as it reduces the possibility of shrinkage during cooling.

To calculate the degree of crystallinity of PI powders, we used the enthalpy of melting ΔH_m determined earlier for R-BAPB with a degree of crystallinity of 100%, which was ~90 J/g [22]. This suggests that the crystallinity degree of polyimide samples obtained by thermal imidization is ~61%, while for chemically imidized powders, it is ~50% (Table I). In accordance with the above, due to the lower crystallinity degree of the polyimide powder obtained by chemical imidization, a lower degree of shrinkage in the SLS process can be expected.

Based on the data obtained by the thermogravimetric analysis (TGA), it can be concluded that all polyimide powders are stable up to the temperature of ~555 °C (the temperature at which a loss of 5% of the polymer mass occurs), after which

TABLE I: Thermophysical properties of the studied R-BAPB powders.

Sample	T_g, °C	T_m, °C	ΔH, J/g	The degree of crystallinity, %	Degradation temperature (weight loss τ_5), °C
R-BAPB therm-imid	199	318	55.2	61	555
R-BAPB chem-imid	200	318	44.5	50	554

Where T_g—glass transition; T_m—melting temperature; ΔH—enthalpy melting.

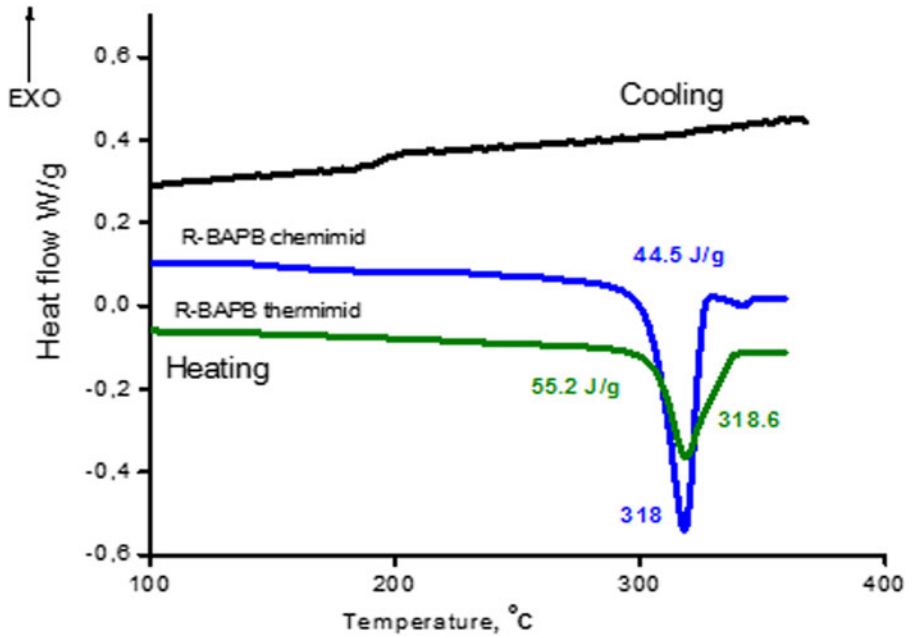


Figure 1: DSC curves of polyimide powders.

https://doi.org/10.1557/jmr.2019.161 Published online by Cambridge University Press

© Materials Research Society 2019

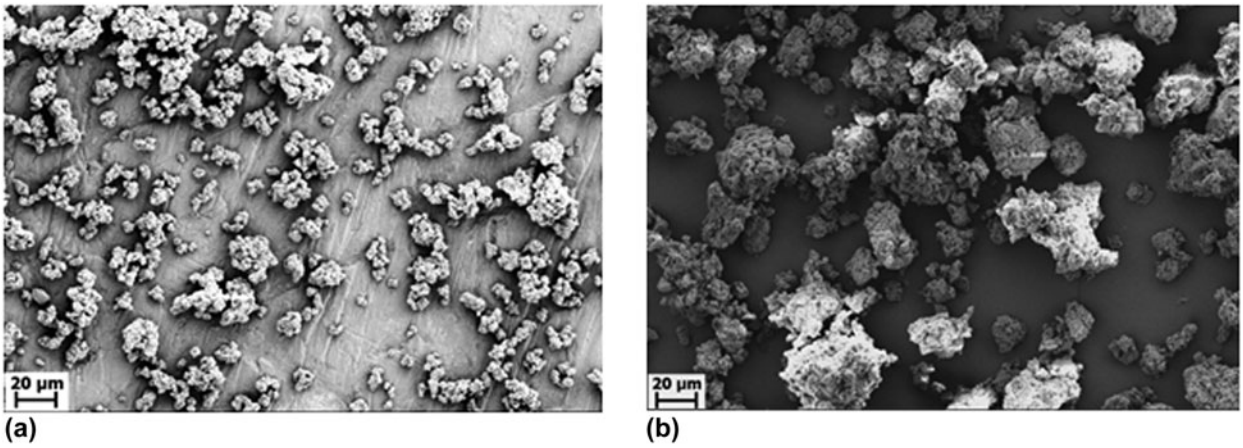


Figure 2: SEM micrographs of powder R-BAPB obtained by the following methods: (a) chemical and (b) thermal imidization.

the thermal decomposition processes begin to activate (Table I). No difference in the beginning of thermal decomposition for polyimide obtained by thermal and by chemical imidization was observed.

Particle shape and particle size distribution are very important volumetric characteristics of the material for SLS. The granulometric properties of the powder used for SLS have a strong influence on the processing, as well as on the final properties of the sintered parts. Too large particles will limit the accuracy of the sintered part, while too small powder particles will tend to agglomerate, and therefore, a good application of the powder layer will be difficult [4].

The study of the shape, size, and fractional composition of the powder was performed by scanning electron microscopy (SEM). Micrographs of the polyimide powder R-BAPB obtained by thermal and chemical imidization are shown in Fig. 2.

To determine the particle size distribution, these micrographs were processed using the "ImageJ" software product. Wherein statistical precise measurements of the particle size of the polyimide powders were carried out for a minimum of 40 SEM micrographs of different places of the sample obtained at a magnification of ×1000 and results are shown in Fig. 3.

The imidization method greatly influences the particle size. R-BAPB obtained by the chemical modification method is characterized by a fairly narrow particle size distribution and the main fraction lies in the range of 6–15 μm. In the case of polyimide obtained by thermal imidization, particles with a large scatter in particle sizes are formed, and the main fraction is 10–40 μm (see Fig. 3). In this case, the morphology of the polyimide powder particles has an irregular shape both in the case of a polyimide powder obtained by thermal and by chemical imidization [Figs. 2(a) and 2(b)].

An important characteristic of powders for laser sintering is bulk density. The higher the bulk density, the greater the possibility of obtaining a defect-free sample. It characterizes the

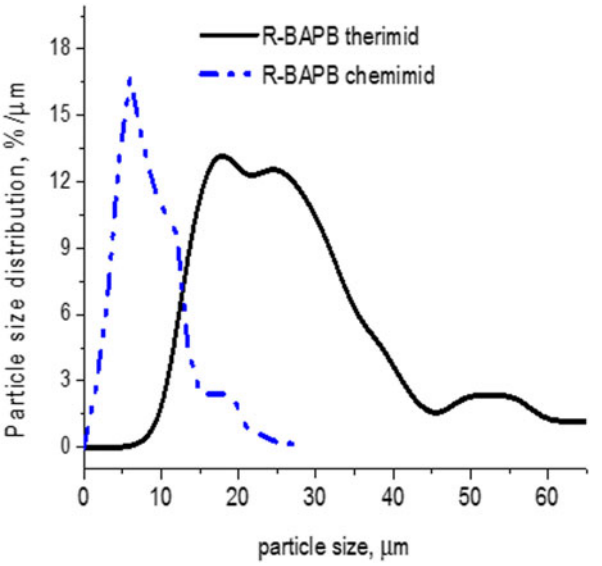


Figure 3: Size distribution of R-BAPB powder particles depending on the method of imidization.

degree of packing of the powder particles when applied in the SLS process. The results of the study of bulk density, depending on the method of production and additional heat treatment of the R-BAPB powder, are presented in Table II. The method of chemical modification allows one to obtain denser powders comparing to the thermally imidized powder. Bulk density of chemically imidized polyimide powders is 40% higher than that of the thermally imidized powder. Besides, due to the additional high-temperature annealing (305 °C) under vacuum (1 mmHg), it is possible to increase the bulk density by 15–30% depending on the method of imidization (Table II). A possible explanation for the difference in bulk density between chemical and thermal imidization is that during chemical imidization, under the action of an imidizing mixture, a more uniform "soft" cyclization of polyamide acid occurs throughout

https://doi.org/10.1557/jmr.2019.161 Published online by Cambridge University Press

© Materials Research Society 2019

its volume, which contributes to the formation of a denser powder. On the contrary, during thermal imidization, there is a certain temperature gradient over the volume of the reaction mixture leading to a powder structure that is as loose as possible.

The fusion of powder particles is of great importance in order to obtain dense polymer materials without the presence of nonmelted domains [23]. A certain melt viscosity is necessary for good fusion of particles. If the viscosity of the polymer is too low, particles can quickly coalescence; however, in this case, a large shrinkage occurs during the sintering process. On the contrary, in polymers with a high molecular weight having a high melt viscosity, the process of particle fusion occurs slowly, but it makes possible to form a material with a higher strength. The process of particle coalescence is particularly influenced by viscosity at low shear rate or zero shear viscosity. Since no mechanical impact is applied on the polymer during laser sintering, unlike standard polymer processing methods such as extrusion, injection molding, and hot pressing, the complete fusion of particles is often limited and high density is difficult to achieve.

TABLE II: Table of values of bulk density of R-BAPB powders.

Sample	Bulk density, g/mL	Bulk density after drying at 305 °C under vacuum 1 h, g/mL
R-BAPB therm-imid	0.160	0.209
R-BAPB chem-imid	0.225	0.282

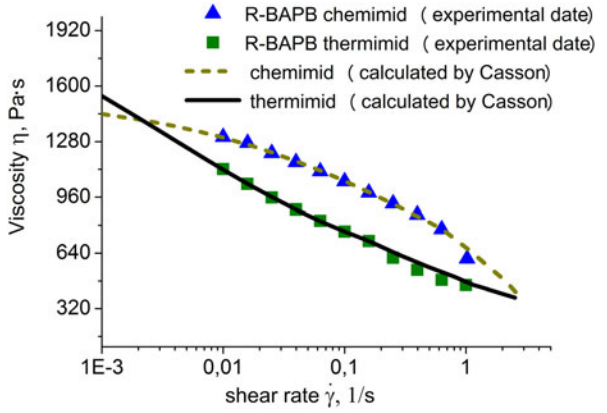


Figure 4: Dependence of the viscosity of R-BAPB melts obtained by chemical and thermal imidization.

To determine the viscosity at zero shear, the rheological curves of the polyimide melts were processed using the Cross model, which describes the rheological behavior of the system, and the parameters of this model were obtained, including the viscosity at zero shear—η_0 (see Fig. 4). The processing was carried out using the following formula:

$$\eta(\dot{\gamma}) = \eta_\infty + \frac{\eta_0 - \eta_\infty}{1 + (\alpha_c \cdot \dot{\gamma})^p} \quad , \tag{1}$$

where $\dot{\gamma}$—shear rate; η_0—zero shear viscosity, Pa s; η_∞—infinite shear viscosity, Pa·s; α—relaxation time, p—exponent (0.4).

When the experimental data were analyzed using Cross equation, it was found that in the case of chemically imidized polyimide value of zero, shear viscosity was 1546 Pa s, which is lower than the thermally imidized powder—2251 Pa s (Fig. 4). This suggests that for the chemically imidized polyimide powder, particle fusion should be easier than for the thermally imidized polyimide.

Among the parameters of laser sintering, the laser power has the greatest effect on the process. For the chemically imidized R-BAPB powder, increasing the laser power from 60 to 67.5 W leads to an increase in the mechanical characteristics of the sintered samples. So with an increase in laser power from 60 to 65 W, the tensile strength is increased by 60% (from 23 to 37 MPa). At 65 W, there is a maximum of mechanical characteristics (Table III). A further increase in the laser power from 65 to 67.5 W practically does not affect the changes in the mechanical characteristics of the sample. When the laser power is increased from 60 to 65 W, apparently, a decrease in the system viscosity appears and, consequently, an increase in the density of the material, which leads to higher mechanical parameters. With a further increase in laser power, no decrease in the system viscosity was observed. At a high power (67 W), the formation of shear deformations is already possible under laser irradiation. These effects can result in a change of the geometry of the sintered objects. This, in turn, will lead to a decrease in the mechanical characteristics of the sample being formed [11].

TABLE III: Mechanical properties of samples obtained by the SLS method based on thermal and chemical imidized R-BAPB powder.

Sample	Laser power, W	σ, MPa	*E*, MPa	ε, %
R-BAPB thermimid	65	14.94 ± 2.22	737 ± 45.2	3.67 ± 0.7
R-BAPB chimimid	65	36.80 ± 2.51	1321 ± 87	5.67 ± 0.89
R-BAPB chimimid	60	23.28 ± 3.37	1190 ± 45	3.17 ± 0.80
R-BAPB chimimid	62.5	25.93 ± 3.37	1121 ± 86	4.21 ± 0.40
R-BAPB chimimid	67.5	34.16 ± 3.71	1314 ± 93	5.67 ± 0.89

Where σ—tensile strength; *E*—tensile modulus; ε—tensile strain.

https://doi.org/10.1557/jmr.2019.161 Published online by Cambridge University Press

© Materials Research Society 2019

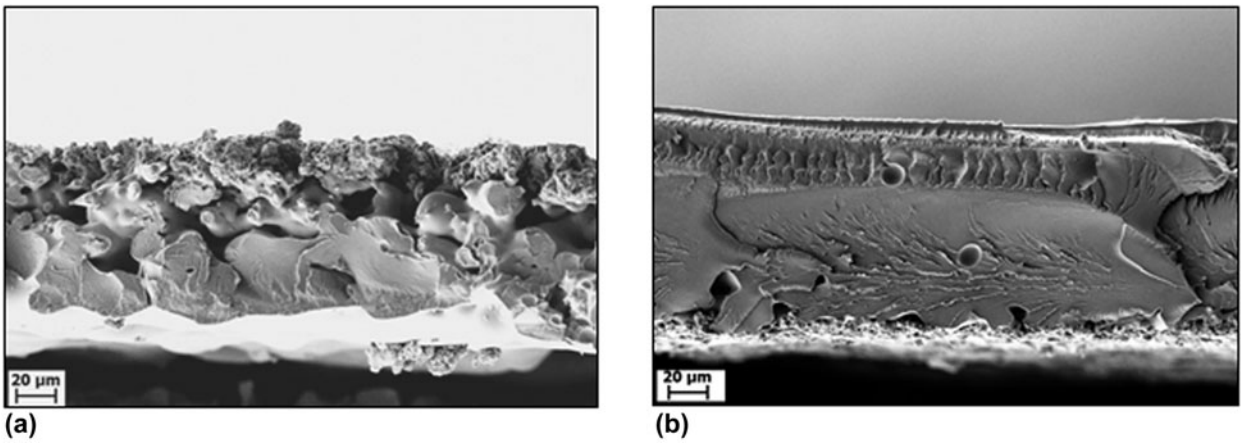


Figure 5: SEM micrographs of the cryo-cleaved polyimide films obtained by the SLS method based on (a) R-BAPB thermimide; (b) R-BAPB chemimide.

As it was discovered, the mechanical characteristics of the films obtained by the SLS method are strongly influenced by the method of imidization of the initial powder (see Table III). In the films obtained from the powder synthesized by the chemical imidization method, higher mechanical characteristics are observed as compared to the sample based on the thermally imidized polyimide. So the tensile strength and elasticity modulus in the samples obtained from the chemically imidized polyimide powder are 2.5 and ~2 times higher than the strength and modulus of the samples from thermally imidized powder, respectively. Such a sharp difference in mechanical characteristics is probably due to the fact that during the process of chemical imidization, a more dense powder was formed. This facilitates the process of particles fusion and the formation of a more dense film structure. This phenomenon is observed in the analysis of SEM micrographs showing the morphology of the destruction surface of polyimide films obtained after laser sintering (Fig. 5). Films about 105 μm thick were formed after sintering. In the samples obtained from polyimide synthesized by the thermal imidization method, the presence of pores in the structure is observed, probably due to the difficulties encountered during the deposition and coalescence of the particles. The formation of such defects in the film structure is probably owing to the low bulk density of the polyimide powder particles. A different picture is observed during sintering of a chemically imidized polyimide powder. In this case, the particles are almost completely coalesced with each other to form a monolithic film [Fig. 5(b)].

Conclusions

In the present work, we conducted a comparative study of the properties of polyimide powders obtained by chemical and by thermal imidizations for further processing using the SLS method. In the case of chemical imidization, more dense polyimide powders were formed with a narrow particle size distribution and a lower crystallinity degree compared to the thermally imidized polyimide powder. On the basis of the synthesized polyimide powders, the samples in the form of films were first obtained by the SLS method. It was found by the SEM method that using chemical imidization leads to formation of more dense and monolithic samples under the action of laser radiation. Studies of the mechanical properties of the obtained films showed that the best characteristics were obtained on samples formed from the chemically imidized polyimide powder with a laser power of 65 W. In general, the perspective of the use of the semi-crystalline heat-resistant thermoplastic polyimide powder for processing it by SLS is shown.

Materials and methods

The following monomers were used to synthesize polyimide: 1,3-bis(3′,4-dicarboxyphenoxy)benzene dianhydride (R dianhydride), T_m ~ 163–165 °C, (OOO TechHimProm, Yaroslavl, Russia), diamine 4,4-bis(aminophenoxy)diphenyl (BAPB), T_m ~ 198–199 °C, manufacturer VWR International (Radnor, Pennsylvania). Phthalic anhydride was chosen as the chain growth limiter during polycondensation. T_m ~ 131–134 °C, Sigma-Aldrich Co., LLC (St. Louis, Missouri). Triethylamine, benzene, and acetic anhydride were obtained by Sigma-Aldrich Co., LLC.

Synthesis of semi-crystalline polyimide based on resorcinol dianhydride R (1,3-bis-(3,3′,4,4′-dicarboxyphenoxy)benzene) and tetracyclic diamine BABP (4,4′-bis(4″-aminophenoxy)biphenyl) was made by chemical and thermal imidization.

The first stage of the synthesis was common for the two methods and included the polycondensation of anhydride R with diamine to polyamic acid (PAA) in a solution of the amide solvent *N*-methylpirrolidone. A certain ratio of dianhydride to diamine was withstood to control the molecular weight. The ratio of the monomers (the molar ratio) of dianhydride to

https://doi.org/10.1557/jmr.2019.161 Published online by Cambridge University Press

© Materials Research Society 2019

diamine was 0.95:1. The resulting PAA was stirred for 4 h; then, a calculated amount of phthalic anhydride was added in the solution in order to break the chain. After additional mixing for 2 h, the initial PAA with terminal phthalamic acid groups was obtained [24, 25, 26, 27]. The resulting prepolymer solution in an amide solvent was converted to polyimide in two different ways: by thermal or by chemical cyclization (imidization) of PAA [28, 29].

The method of thermal imidization includes cyclization of PAA units in the solution of a prepolymer in *N*-methylpyrrolidone (MP) with an increase of temperature from 130 °C to 190 °C at a rate of 5 °C/min. To accelerate the imidization reaction of PAA and its complete conversion to polyimide, the released imidization water was removed from the synthesis zone as a toluene-water azeotrope. The resulting polyimide was isolated as a fine powder. Using N-MP treatment, nonreactive or incompletely imidized low-molecular-weight monomers were washed out from the synthesized polyimide powder, and then the isolated powders were washed in methyl alcohol. Further, the polymer powders were dried in vacuum, at a temperature of 220 °C for 2 h [29].

The method of chemical imidization includes the cyclization of PAA units in the solution of a prepolymer in N MP with chemical agents of an imidizing mixture. The imidizing mixture was a freshly prepared solution of three components: acetic anhydride, triethylamine, and benzene. The composition was obtained so that the molar ratio of acetic anhydride and triethylamine to the molar ratio of PAA was 3:1, and the molar ratio of benzene to PAA, respectively, 1:1. Chemical imidization of PAA was made with vigorous stirring for 1.5 h at room temperature until the powdery precipitate appeared in solution. This powdery precipitate was cooled to room temperature, filtered through a Schott filter, and washed with ether and methyl alcohol. After that, the polyimide powder was heated at 220 °C for 2 h [28, 29]. In this case, the IR-spectra are identical for powders obtained by thermal and chemical imidization.

FTIR spectra were recorded on Bruker Vertex 70, using ATR-attachment; Zn–Se crystals (reflection angle 45°) were used as reflection components.

To determine the size, morphology, and size distribution of the powder R-BAPB, as well as to study the structural changes occurring in two-dimensional samples (films) obtained after SLS, scanning electron microscopy (SEM) was used. These studies were performed using a SUPRA 55VP scanning electron microscope (Carl Zeiss, Munich, Germany). To analyze the structure of the film after sintering, a transverse cleavage was made in liquid nitrogen. Before placing the samples inside the microscope chamber, a thin conducting layer of gold or platinum was deposited on their surface. Accelerating voltage was 3–5 kV. The bulk density of the polymer powder composition was determined according to ISO 60-77.

The melt viscosity was studied on an Anton Paar Physica MCR301 rheometer in the measuring unit cone-plane CP25-2 (diameter 25 mm, angle 2°, gap between cone and plane 0.05 mm) at a temperature of 360 °C. The test was carried out in shear mode at a shear rate from 1 to 0.01 s^{-1}.

The study of the thermophysical properties of polyimide R-BAPB powders obtained both by thermal and by chemical imidization was carried out using the methods of thermal analysis with the help of Netzsch device (Selb, Germany)—DSC 204 F1 (differential scanning calorimetry, DSC). The tests were carried out on powders in the temperature range from 30 to 400 °C. All samples were loaded in triplicate at a heating rate of 10 °C/min, in an inert atmosphere (argon). Netzsch Proteus® software (Russia, Moscow) was used to determine the enthalpy of melting ΔH_m, melting point T_m, and glass transition temperature T_g.

Thermogravimetric analysis (TGA) was carried out by TG 209 F1 device (Netzsch, Germany). The tests were carried out in the temperature range from 30 to 700 °C at a heating rate of 10 °C/min, in an inert atmosphere (argon).

Laboratory samples were obtained by laser sintering based on the polymide powders in the form of 50 × 20 mm films on an STARSHAPE C experimental setup with a CO_2 laser with a wavelength of 10,600 nm, a scanning speed of 2000 mm/s and a power from 60 to 67.5 W.

Mechanical tests were carried out using the universal tensile testing machine INSTRON 5943 (High Wycombe, U.K.). The test speed was 1 mm/min. The base length for film samples was 20 mm and the width of 2 mm and the data acquisition rate was 0.01%. From the obtained tension diagrams, the values of strength, modulus under tension, and deformation were calculated.

Acknowledgments

The present study has been supported by the Russian Foundation for Basic Research (Grant No. 17-03-00733A).

References

1. **I. Gibson, D. Rosen, and B. Stucker**: *Additive Manufacturing Technologies: Rapid Prototyping to Direct Digital Manufacturing* (Springer Science and Business Media, New York, 2010); p. 472.
2. **B. Wendel, D. Rietzel, F. Kuhnlein, R. Feulner, G. Hulder, and E. Schmachtenberg**: Additive processing of polymers. *Macromol. Mater. Eng.* **293**, 799 (2008).
3. **S. Yang and J. Evans**: Metering and dispensing of powder; the quest for new solid freeforming techniques. *Powder Technol.* **178**, 56 (2007).
4. **S. Berretta, O. Ghita, and K.E. Evans**: Morphology of polymeric powders in Laser Sintering (LS): From Polyamide to new PEEK powders. *Eur. Polym. J.* **59**, 218 (2014).

https://doi.org/10.1557/jmr.2019.161 Published online by Cambridge University Press

© Materials Research Society 2019

5. **S. Dupin, O. Lame, C. Barrès, and J.Y. Charmeau**: Microstructural origin of physical and mechanical properties of polyamide 12 processed by laser sintering. *Eur. Polym. J.* **48**, 1611 (2012).
6. **M. Vasquez, B. Haworth, and N. Hopkinson**: Methods for quantifying the stable sintering region in laser sintered polyamide-12. *Polym. Eng. Sci.* **53**, 1230 (2013).
7. **Y. Guo, K. Jiang, and D.L. Bourell**: Preparation and laser sintering of limestone PA12 composite. *Polym. Test.* **37**, 210 (2014).
8. **R.D. Goodridge, C.J. Tuck, and R.J.M. Hague**: Laser sintering of polyamides and other polymers. *Prog. Mater. Sci.* **57**, 229 (2012).
9. **S.C. Lao, W. Yong, K. Nguyen, T.J. Moon, J.H. Koo, L. Pilato, and G. Wissler**: Flame-retardant polyamide 11 and 12 nanocomposites: Processing, morphology, and mechanical properties. *J. Compos. Mater.* **44**, 2933 (2010).
10. **W. Zhou, X. Wang, J. Hu, and X. Zhu**: Melting process and mechanics on laser sintering of single layer polyamide 6 powder. *Int. J. Adv. Manuf. Technol.* **69**, 901 (2013).
11. **B. Caulfield, P.E. McHugh, and S. Lohfeld**: Dependence of mechanical properties of polyamide components on build parameters in the SLS process. *J. Mater. Process. Technol.* **182**, 477 (2007).
12. **Y. Shi, Y. Wang, J. Chen, and S. Huang**: Experimental investigation into the selective laser sintering of high-impact polystyrene. *J. Appl. Polym. Sci.* **108**, 535 (2008).
13. **Y. Shi, J. Chen, Y. Wang, Z. Li, and S. Huang**: Study of the selective laser sintering of polycarbonate and postprocess for parts reinforcement. *J. Mater.: Des. Appl.* **221**, 37 (2007).
14. **O. Ghita, E. James, R. Davies, S. Berretta, B. Singh, S. Flint, and K.E. Evans**: High Temperature Laser Sintering (HT-LS): An investigation into mechanical properties and shrinkage characteristics of Poly(Ether Ketone) (PEK) structures. *Mater. Des.* **61**, 124 (2014).
15. **O.R. Ghita, E. James, R. Trimble, and K.E. Evans**: Physico-chemical behaviour of Poly(Ether Ketone) (PEK) in High Temperature Laser Sintering (HT-LS). *J. Mater. Process. Technol.* **214**, 969 (2014).
16. **S. Berretta, K.E. Evans, and O. Ghita**: Processability of PEEK, a new polymer for high temperature laser sintering (HT-LS). *Eur. Polym. J.* **68**, 243 (2015).
17. **M. Schmidt, D. Pohle, and T. Rechtenwald**: Selective laser sintering of PEEK. *CIRP Ann.* **56**, 205 (2007).
18. **T.A. Kostereva, Y.U.N. Panov, A.L. Didenko, I.G. Silinskaya, V.M. Svetlichnyi, V.E. Yudin, and V.V. Kudryavtsev**: Controlling the viscosity of melts of partially crystalline polyimides used for preparing carbon-reinforced plastics. *Russ. J. Appl. Chem.* **77**, 1355 (2004).
19. **L. Fiedler, L. Osvaldo, G. Correa, H. Radusch, A. Wutzler, and J. Gerken**: Evaluation of polypropylene powder grades in consideration of the laser sintering processability. *J. Plast. Technol.* **3**, 4 (2007).
20. **A.L. Didenko**: Composition of semi-crystalline polyimides based on bis(4-aminophenoxy)biphenyl are binders for carbon fiber composite. Thesis, IMC RAS, Saint-Petersburg, 2004; p. 134.
21. **V.E. Yudin and V.M. Svetlichnyi**: Carbon plastics based on thermoplastic polyimide binders modified with nanoparticles. *Polym. Sci., Ser. C* **58**, 16–25 (2016).
22. **V.E. Yudin, V.M. Svetlichnyi, G.N. Gubanova, A.L. Didenko, E.N. Popova, T.E. Sukhanova, A.I. Grogoriev, and T.A. Kostereva**: Influence of crystallinity of R-BAPB-Type polyimide matrix on the thermal and mechanical properties of carbon fiber reinforced composites. In *Polyimides and Other High Temperature Polymers*, Vol. **3**, K.L. Mittal, ed. (Plenum Press, New York, 2005); p. 229.
23. **Y. Shi, Z. Li, H. Sun, S. Huang, and F. Zeng**: Effect of the properties of the polymer materials on the quality of selective laser sintering parts. *Proc. Inst. Mech. Eng., Part L* **218**, 247 (2004).
24. **M.I. Bessonov, M.M. Koton, V.V. Kudryavtsev, and L.A. Laius**: *Polyimides-Thermally Stable Polymers* (Plenum, New York, 1987); p. 328.
25. **S. Srinivas, M. Graham, M.H. Brink, S. Gardner, R.M. Davis, J.E. McGrath, and G.L. Wilkes**: Influence of melt stability on the crystallization of bis(4-aminophenoxy)benzene-oxydiphthalic anhydride based polyimides. *Polym. Eng. Sci.* **36**, 928 (1996).
26. **V.V. Nesterov, V.V. Kudryavtsev, V.M. Svetlichnyi, N.V. Gazdina, N.G. Belnikevich, O.I. Kurenbin, and T.I. Zhukova**: Study of soluble polyamic acids and polyester imides by methods of exclusion liquid chromatography. *Polym. Sci., Ser. A* **39**, 1387 (1997).
27. **G.A. Polotskaya, Y.P. Kuzhnetsov, A.V. Anikin, N.V. Lukashova, T.I. Zhukova, V.M. Svetlichnyi, V.V. Kudryavtsev, and M.A. Eremina**: Chemical-structure and gas-separating properties of aromatic polyesterimides membranes. *Polym. Sci., Ser. A* **34**, 107 (1992).
28. **V.E. Yudin, A.G. Kalbin, T.K. Meleshko, A.I. Grigor'ev, G.N. Gubanova, N.N. Bogorad, Y.N. Panov, O.F. Pozdnyakov, B.P. Redkov, A.O. Pozdnyakov, and V.V. Kudryavtsev**: Features of the crystal structure of the polyimide derived from 3,3′-diaminobenzophenone and 3,3′,4,4′-benzophenonetetracarboxylic dianhydride. *Russ. J. Appl. Chem.* **74**, 1183 (2001).
29. **V.E. Yudin, J.U. Otaigbe, L.T. Drzal, and V.M. Svetlichnyi**: Novel semicrystalline thermoplastic r-bapb type polyimide matrix reinforced by graphite nanoplatelets and carbon nanoparticles. *Adv. Compos. Lett.* **15**, 137 (2006).

https://doi.org/10.1557/jmr.2019.161 Published online by Cambridge University Press

© Materials Research Society 2019